JACS
JOURNAL OF THE AMERICAN CHEMICAL SOCIETY

COMMUNICATION

pubs.acs.org/JACS

Observations of PDDTT Subject to Thermal Treatment: Correlation between Performance and Order

Jonathan D. Yuen,[*,†] Rajeev Kumar,[†,§,∥] Jason Seifter,[†,∥] Sebastian Valouch,[†,‡] Dante Zakhidov,[†] Daniel Moses,[†] Uli Lemmer,[‡] Alan J. Heeger,[†] and Fred Wudl[*,†]

[†]Center for Polymers and Organic Solids, University of California, Santa Barbara, California 93106, United States

[‡]Light Technology Institute, Karlsruhe Institute of Technology, Kaiserstrasse 12, 76131 Karlsruhe, Germany

Supporting Information

ABSTRACT: We show that polybis(thienyl)thienodiathiazolethiophene (PDDTT), a high-performance semiconducting polymer for photodetectors and field-effect transistors, has strong performance dependence on annealing temperature. An unprecedented increase of 3 orders of magnitude is observed in both transistor and photoconductive properties. XRD and AFM evidence points to increased ordering in PDDTT films with annealing. This correlation highlights the importance that order has in determining performance in PDDTT and has possible implications in the design of polymers.

Conjugated polymer semiconductors are promising candidates as active layers for low-cost, flexible electronics due to their solution processablity, mechanical flexibility, compatibility with thermally sensitive substrates, and electronic tunability.[1] Their utility in organic field-effect transistors (FETs) has been buoyed by recent reports of mobilities approaching or exceeding 1 $cm^2\ V^{-1}\ s^{-1}$,[2] the benchmark mobility for amorphous Si thin-film FETs. Despite considerable improvements in the performance of conjugated polymer semiconductors, more work has to be done to enhance their performance.

Control of morphology is widely acknowledged to be essential in achieving high performance in polymer FETs,[3] particularly with regards to the role of order. Until recently, experimental evidence generally indicated that high crystallinity was necessary for good transport in polymer FETs.[4] However, it is also known that good mobilities in amorphous polymer FETs have been around 10^{-2} $cm^2\ V^{-1}\ s^{-1}$,[5] a level comparable to that of crystalline low-molecular-weight polymers.[6] Moreover, recent reports have shown that very high mobility can nonetheless be achieved in fairly disordered materials via immediate interchain interactions.[7]

We have observed in situ thermally induced improvement in transistor performance of the donor−acceptor polymer PDDTT (Figure 1a, inset) with strong correlation to ordering, providing insight on the role of order in the device performance of PDDTT. An in situ observation has advantages over an ex-situ experiment: a sample-to-sample comparison based on a sequential chemical or process modification, as external factors beyond ordering that affect performance (such as molecular weight or film thickness) are decoupled from it. This in situ improvement correlated well with the improvement in photoconductivity, indicating that the improvements have both bulk and surface effects. The high performance of PDDTT IR photodetectors has been reported,[8] but not the FET performance. We report high-performance p-type FETs with mobilities above 0.1 $cm^2\ V^{-1}\ s^{-1}$ for thermally optimized films of PDDTT and explain how morphology is critical in achieving high performance.

The synthesis of a PDDTT analogue has been described previously.[8] However, instead of conventional heating methods, we employed microwave heating in chlorobenzene during synthesis, resulting in polymers with 3 times the molecular weight synthesized in less than 1% of the time. In our current synthesis, we used a dodecyl side chain on thiophene instead of a hexyl chain to increase the solubility and processability of PDDTT. A synthesis scheme and comparisons of the variations in synthesis method are shown in Scheme S1 and Table S1 in the Supporting Information, respectively. Because molecular weight generally has a positive correlation with transistor performance,[6,7a] the resulting high molecular weight of PDDTT made it a strong candidate for high-performance FETs. Bottom-gate, Au bottom-contact FETs were patterned on highly doped silicon substrates with a 200 nm SiO_2 dielectric layer passivated with decyltrichlorosilane (DTS). PDDTT was spin-cast from chloroform (CF), chlorobenzene (CB), or orthodichlorobenzene (ODCB) solutions, directly dropped onto the spinning substrate. We observed little variation in FET performance among the solvents used. All samples were dried at 60 °C for 0.5 h after casting and subsequently were annealed for 10 min at each temperature prior to testing.

Transfer curves, both linear source-drain current (I_{SD}) and $|I_{DS}|^{1/2}$, of an FET with PDDTT cast from CB are shown in Figure 1a. Multiple curves were taken at several annealing steps with the source-drain voltage (V_{SD}) at −60 V. We observed steady improvement in FET performance, shown by the rise in current with temperature for gate voltages (V_G) < 0 V. For V_G = −80 V, I_{SD} improved from 2 μA after annealing at 60 °C to 2 mA at 220 °C, an increase in 3 *orders of magnitude*. Output curves of the FET annealed at 220 °C in Figure S1 in the Supporting Information show excellent performance, as reported. Current was not observed after the device was annealed at 250 °C, due to chemical degradation of PDDTT, as shown by thermogravimetric analysis (Figure S2 in the Supporting Information).

To more accurately quantify and compare FET performance with annealing temperature, mobilities (μ) were determined from $\partial|I_{DS}|^{1/2}/\partial V_G$ of the standard equation describing metal−oxide FETs operating in the saturation regime: $I_{DS} = 1/2(W/L)\mu C_i(V_G - V_T)^2$.

Received: August 13, 2011
Published: November 15, 2011

ACS Publications © 2011 American Chemical Society

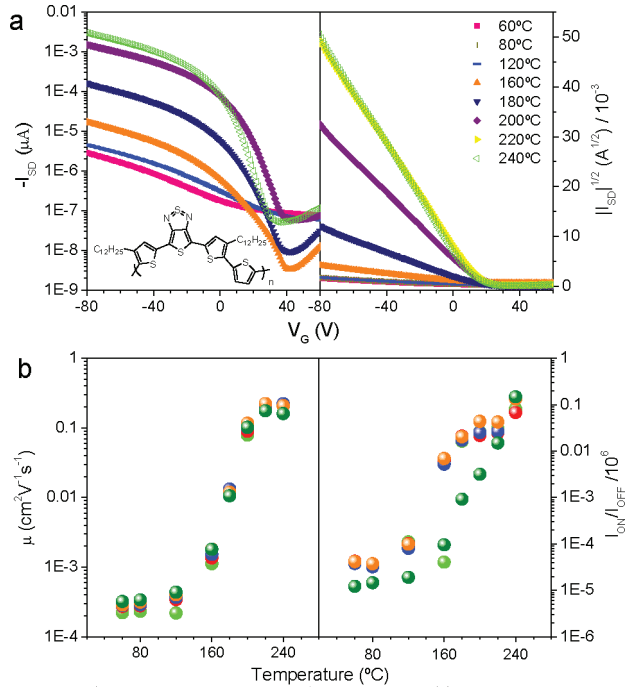

Figure 1. (a) FET transfer curves (I_{SD} and $|I_{SD}|^{1/2}$) at various annealing temperatures, with the PDDTT chemical structure in the inset. (b) Mobility and on−off ratio vs annealing temperature for a set of five FETs.

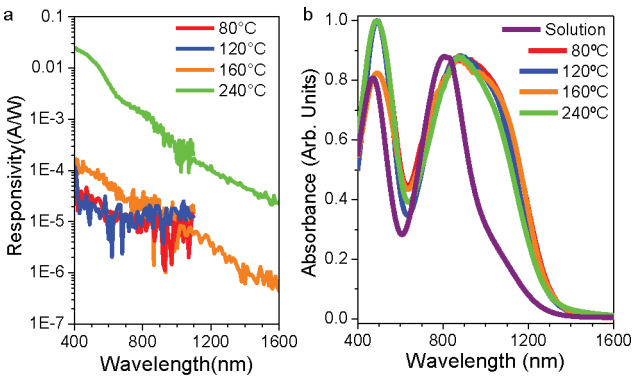

Figure 2. (a) Photoresponsivities and (b) absorption spectra for PDDTT films annealed at various temperatures, with the PDDTT solution spectrum in ODCB plotted in (b).

We note in Figure 1a the excellent fit of $|I_{DS}|^{1/2}$ with the FET model described above, with linear dependence on V_G at all temperatures for all V_G beyond the threshold voltage V_T. The excellent linearity over such a wide range is truly impressive, rare even for high-performance materials. Mobilities (μ) of five devices were plotted against annealing temperature in Figure 1b. We observed that mobilities remained around 10^{-4} cm^2 V^{-1} s^{-1} from 60 to 120 °C. A steady rise occurred beyond that, hitting a plateau above 10^{-1} cm^2 V^{-1} s^{-1} just after 200 °C. For all devices, the change in μ precisely scales with the increase in I_{SD} in Figure 1a. In both, an increase of 3 orders of magnitude is observed. Despite an extensive search through the literature, we have not been able to find any reports of improvement in p-type mobility as large as what we observed for PDDTT.

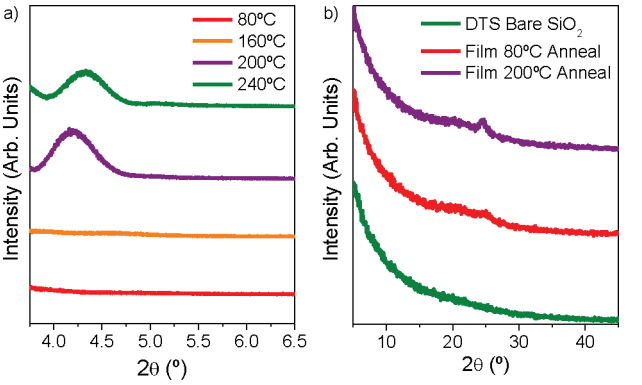

Figure 3. (a) Out-of-plane specular and (b) in-plane grazing incidence XRD spectra for PDDTT films cast on DTS-passivated SiO_2, annealed at various temperatures.

The significant improvement in PDDTT FET performance with annealing temperature is not only limited to mobility. Figure 1b also plots FET on−off ratios (I_{ON}/I_{OFF}) with annealing temperature for the same devices. The dependence of I_{ON}/I_{OFF} with annealing essentially follows that of mobility, with a low plateau just before 120 °C and a high plateau after 200 °C. All benchmarks of FET performance, I_{SD}, μ, and I_{ON}/I_{OFF}, show the same dependence with annealing temperature.

Annealing temperature also affected the photoconductive properties of PDDTT. Figure 2a shows plots of the photoconductive response of samples of neat PDDTT with different annealing temperatures. Again, photoresponsivity scales with the other benchmarks described above, with negligible responsivity when annealed below 120 °C and a slight jump at 160 °C, followed by a significant jump in photoresponse after the sample was annealed at 240 °C. In particular, at λ = 500 nm, the photoresponse jumps 3 orders of magnitude from 10^{-5} A/W with annealing at 80 °C to 10^{-2} A/W at 240 °C. We note that, although strong photoresponsivity was not observed in the infrared in neat PDDTT films, blending with PCBM resulted in high infrared responsivity.[8] Although it may be argued that the improvement in photoresponse could be due to improvement in the absorption properties of PDDTT, we show that this is not the case. Figure 2b shows the absorption spectra of PDDTT dissolved in ODCB and PDDTT films on quartz annealed at different temperatures. No significant shift in absorption is observed in PDDTT films with annealing, indicating that the improvement in photoresponse is not due to photophysical properties, but rather, transport-related. In contrast, a bathochromic spectral widening occurs from solution to film, with development of a red shifted shoulder related to increased interchain interactions in the solid state, such as $\pi-\pi$ stacking.[9]

The observation that improvement in photoresponse is congruent with improvement observed in FET properties is highly significant. Transport within an FET is limited to the semiconductor−dielectric interface, whereas photoconductivity is a bulk effect. The improvement from annealing affects PDDTT as a material in general, both equally in the bulk and at the surface. Therefore, subsequent correlations of performance with morphology are definitely within context.

We describe X-ray diffraction (XRD) and atomic force microscopy (AFM) measurements of PDDTT, correlating morphology with performance. Figure 3a shows out-of-plane specular diffractograms of PDDTT films spin-cast on DTS-passivated

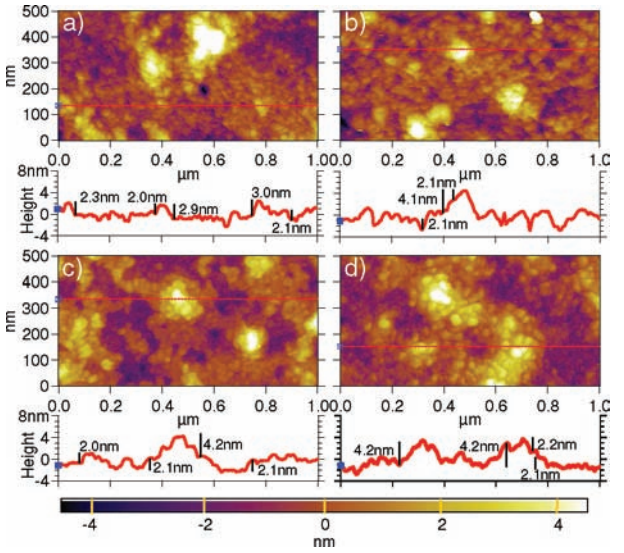

Figure 4. AFM images for PDDTT films cast on DTS-passivated SiO_2 annealed at (a) 80, (b) 160, (c) 200, and (d) 240 °C. For each section, the top is the surface image and the bottom is the topology profile of a section of the surface image above, as outlined by the red line. All images and profiles share the same scaling with each other.

oxidized silicon substrates annealed at various temperatures. At 80 and 160 °C, no peaks are observed, but at 200 °C, a peak centered at $2\theta = 4.2°$ appears, shifting slightly at 240 °C to $2\theta = 4.3°$. This scattering feature can be assigned to alignment of polymer sheets parallel to the surface, with an intersheet spacing around 2.1 nm at 200 °C and 2 nm at 240 °C, similar to that of RR-P3HT and other polymers.[4,7b,10,11] Additional peaks observed below 3.5° are Kiessig fringes, as described in the Supporting Information.

Thermally induced ordering can also be observed via in-plane grazing incidence XRD, as shown in Figure 3b. Diffractograms of a bare substrate, a PDDTT-covered substrate annealed at 80 °C, and another annealed at 200 °C, all DTS-passivated, are compared. Out-of-plane measurements were performed, and the resulting XRD spectra corroborated with specular spectra. No peaks were observed for the bare substrate, but for the PDDTT film annealed at 80 °C, a shallow peak around $2\theta = 25°$ was observed, increasing for the sample annealed at 200 °C. This corresponds to a length scale of around 3.5 Å, a typical length scale of $\pi-\pi$ stacking in conjugated polymers.[4] This indicates that $\pi-\pi$ stacking already exists at 80 °C, albeit sparse, shown by the shallow peak. The increase of the peak at 200 °C is due to expansion of π-stacked regions, indicating that the polymer sheets that form at 200 °C also consist of π-stacked polymer chains. Thus, we can infer from both measurements that annealing results in increased ordering from the evolution of π-stacked polymers sheets.

AFM measurements of surface morphology on similar samples annealed at the same temperatures as in the XRD are shown in Figure 4. Topology profiles of a segment of each AFM image (delineated by a red line) are included. Additional images in Figure S4 and calculated height distributions (Figure S5) are available in the Supporting Information. At 80 °C (Figure 4a), we observed a film of uniformly distributed, polymeric nodules. At 160 °C (Figure 4b), grain ripening was observed, correlating with the slight increase in transport observed in other experiments. Height distributions at 80 and 160 °C showed no significant features. At 200 °C (Figure 4c), where strong improvement in transport was observed, a significant change in morphology also occurred. Nodules aggregated to form terrace structures, as shown by the high color contrast due to height differences between terraces. From the height histogram, the terrace height was determined to be around 2.1 nm, corresponding well to step features measured in the topology profile and to the spacing length determined in XRD. This confirms that the terraces are formed due to the stacking of molecular sheets. At 240 °C (Figure 4d), loss in color contrast indicated that the terraces have coalesced and individual nodules are observed again. This possibly explains the decrease in separation length from 200 to 240 °C observed in XRD. The height distribution at 240 °C showed no significant features.

Comparing morphology with the performance of PDDTT in this experiment, we see that the disorder-to-order transition, that is, the evolution of π-aligned, vertically stacked polymer sheets from disordered polymer nodules, is intimately related to the substantial increase in FET performance and photoresponsivity in PDDTT, indicating that ordering is critical for good performance for PDDTT. This rather intuitive observation, however, has not been commonly observed in polymer semiconductors. Indeed, it is generally observed that little variation in mobility occurs in polymer FETs through in situ experiments.[10a,12] Samples subject to either solvent annealing or thermal processing typically show improvement in mobilities generally within 1 order of magnitude, up to a maximum of 2 orders of magnitude, sometimes despite large morphological variations. This is mainly due to pre-existing order in as-cast films of polymers that show thermally induced structural transitions, such as liquid crystalline polymers.[4d−g] A more accurate corollary would be based on observations of P3HT. While P3HT has no thermally induced structural transitions, solvent-induced structural variations can be achieved and a similar correlation with order and performance can be observed.[4b,6] Thus, we believe that the properties of PDDTT are nonetheless similar to those of many other polymers and can be applied toward the better design of polymers with high performance.

In conclusion, good correlation between morphological variations and device performance in PDDTT was determined via thermally annealed samples. We find that up to 3 orders of magnitude in improvement can be observed in current, mobility, and on−off ratio in PDDTT FETs, and in photoresponse in neat films of PDDTT. We observe that annealing causes polymer nodules that make up as-cast PDDTT to form π-aligned polymer sheets, stacked parallel to the substrate. We conclude that structural and morphological ordering are critical determinants of high performance in PDDTT, and such factors should be taken into consideration when designing polymers with improved performance.

■ ASSOCIATED CONTENT

Ⓢ Supporting Information. Experimental methods, synthesis comparisons (Table S1), FET (Figure S1) and TGA (Figure S2) data, XRD (Figure S3) and AFM (Figures S4 and S5) discussions, and a complete reference list are available in the Supporting Information. This material is available free of charge via the Internet at http://pubs.acs.org.

■ AUTHOR INFORMATION

Corresponding Author
djy@engr.ucsb.edu; wudl@chem.ucsb.edu

Present Addresses
[§]Nano-Terra, Inc., Brighton, MA 02139.

Author Contributions
[||]These authors contributed equally.

■ ACKNOWLEDGMENT

Research was supported by the NSF Polymer program (Grant No. NSF-DMR-0856060). Support for R.K. was through the Center for Energy Efficient Materials (CEEM) supported by the DOE as an EFRC (DE-SC0001009). A portion of this work was done in the UCSB nanofabrication facility, part of the NSF-funded NNIN network. Support for S.V. was through the DFG Center for Functional Nanostructures (CFN), project number A4.2, and the Karlsruhe House of Young Scientists (KHYS). J.D.Y. thanks N. Banerji, G. Hernandez-Sosa, W. L. Leong, C. Takacs, and Y. M. Sun for useful discussions. R.K. thanks K. Brosten for helping in synthesis.

■ REFERENCES

(1) (a) Klauk, H. *Chem. Soc. Rev.* **2010**, *39*, 2643–2666. (b) Gelinck, G.; Heremans, P.; Nomoto, K.; Anthopoulos, T. D. *Adv. Mater.* **2010**, *22*, 3778–3798. (c) Arias, A. C.; MacKenzie, J. D.; McCulloch, I.; Rivnay, J.; Salleo, A. *Chem. Rev.* **2010**, *110*, 3–24.

(2) (a) Yan, H.; Chen, Z.; Zheng, Y.; Newman, C.; Quinn, J.; Dotz, F.; Kastler, M.; Facchetti, A. *Nature* **2009**, *457*, 679–686. (b) Li, Y.; Singh, S. P.; Sonar, P. *Adv. Mater.* **2010**, *22*, 4862–4866. (c) Zhang, W.; Smith, J.; Watkins, S. E.; Gysel, R.; McGehee, M.; Salleo, A.; Kirkpatrick, J.; Ashraf, S.; Anthopoulos, T.; Heeney, M.; McCulloch, I. *J. Am. Chem. Soc.* **2010**, *132*, 11437–11439. (d) Tsao, H. N.; Cho, D. M.; Park, I.; Hansen, M. R.; Mavrinskiy, A.; Yoon, D. Y.; Graf, R.; Pisula, W.; Spiess, H. W.; Müllen, K. *J. Am. Chem. Soc.* **2011**, *133*, 2605–2612.

(3) (a) Jaiswal, M.; Menon, R. *Polym. Int.* **2006**, *55*, 1371–1384. (b) McCulloch, I.; et al. *Adv. Mater.* **2009**, *21*, 1091–1109. (c) Tsao, H. N.; Müllen, K. *Chem. Soc. Rev.* **2010**, *39*, 2372. (d) Salleo, A.; Kline, R. J.; DeLongchamp, D. M.; Chabinyc, M. L. *Adv. Mater.* **2010**, *22*, 3812–3838.

(4) (a) Sirringhaus, H.; Brown, P. J.; Friend, R. H.; Nielsen, M. M.; Bechgaard, K.; Langeveld-Voss, B. M. W.; Spiering, A. J. H.; Janssen, R. A. J.; Meijer, E. W.; Herwig, P.; de Leeuw, D. M. *Nature* **1999**, *401*, 685–688. (b) Surin, M.; Leclère, P.; Lazzaroni, J.; Yuen, J. D.; Wang, G.; Moses, D.; Heeger, A. J.; Cho, S.; Lee, K. *J. Appl. Phys.* **2006**, *100*, 033712. (c) Kline, R. J.; McGehee, M. D.; Toney, M. F. *Nat. Mater.***2006**, *5*, 222–228. (d) McCulloch, I.; Heeney, M.; Bailey, C.; Genevicius, K.; MacDonald, I.; Shkunov, M.; Sparrowe, D.; Tierney, S.; Wagner, R.; Zhang, W.; Chabinyc, M. L.; Kline, R. J.; McGehee, M. D.; Toney, M. F. *Nat. Mater.* **2006**, *5*, 328–333. (e) Li, Y.; Wu, Y.; Liu, P.; Birau, M.; Pan, H.; Ong, B. *Adv. Mater.* **2006**, *18*, 3029–30. (f) Fong, H. H.; Pozdin, V. A.; Amassian, A.; Malliaras, G. G.; Smilgies, D.; He, M.; Gasper, S.; Zhang, F.; Sorensen, M. *J. Am. Chem. Soc.* **2008**, *130*, 13202–13203. (g) Kim, D. H.; Lee, B. L.; Moon, H.; Kang, H. M.; Jeong, E. J.; Park, J. I.; Han, K. M.; Lee, S.; Yoo, B. W.; Koo, B. W.; Kim, J. Y.; Lee, W. H.; Cho, K.; Becerril, H. A.; Bao, Z. *J. Am. Chem. Soc.* **2009**, *131*, 6124–6132.

(5) (a) Veres, J.; Ogier, S.; Leeming, S.; Cupertino, D.; Mohialdin Khaffaf, S. *Adv. Funct. Mater.* **2003**, *13*, 199–204. (b) Veres, J.; Ogier, S.; Lloyd, G.; de Leeuw, D. *Chem. Mater.* **2004**, *16*, 4543–4555. (c) Chung, D. S.; Lee, S. J.; Park, J. W.; Choi, D. B.; Lee, D. H.; Park, J. W.; Shin, S. C.; Kim, Y.; Kwon, S.; Park, C. E. *Chem. Mater.* **2008**, *20*, 3450–3456. (d) Kong, H.; Lee, D. H.; Seo, J.; Oh, J.; Chung, D. S.; Park, J.; Kwon, S.; Lee, Y. S.; Park, C. E.; Shim, H. *ACS Appl. Mater. Interfaces* **2010**, *2*, 1100–1106.

(6) (a) Kline, R. J.; McGehee, M. D.; Kadnikova, E. N.; Liu, J.; Fréchet, J. M. J.; Toney, M. F. *Macromolecules* **2005**, *38*, 3312–3319. (b) Verilhac, J.; LeBlevennec, G.; Djurado, D.; Rieutord, F.; Chouiki, M.; Travers, J.; Pron, A. *Synth. Met.* **2006**, *156*, 815–823. (c) Pingel, P.; Zen, A.; Neher, D.; Lieberwirth, I.; Wegner, G.; Allard, S.; Scherf, U. *Appl. Phys. A: Mater. Sci. Process.* **2008**, *95*, 67–72.

(7) (a) Zhang, M.; Tsao, H. N.; Pisula, W.; Yang, C.; Mishra, A. K.; Müllen, K. *J. Am. Chem. Soc.* **2007**, *129*, 3472–3473. (b) Liu, J.; Zhang, R.; Sauvé, G.; Kowalewski, T.; McCullough, R. D. *J. Am. Chem. Soc.* **2008**, *130*, 13167–13176. (c) Osaka, I.; Zhang, R.; Sauvé, G.; Smilgies, D.; Kowalewski, T.; McCullough, R. D. *J. Am. Chem. Soc.* **2009**, *131*, 2521–2529.

(8) (a) Xia, Y.; Wang, L.; Deng, X.; Li, D.; Zhu, X.; Cao, Y. *Appl. Phys. Lett.* **2006**, *89*, 081106. (b) Gong, X.; Tong, M.; Xia, Y.; Cai, W.; Moon, J. S.; Cao, Y.; Yu, G.; Shieh, C.; Nilsson, B.; Heeger, A. J. *Science* **2009**, *325*, 1665–1667.

(9) (a) Yue, S.; Berry, G. C.; McCullough, R. D. *Macromolecules* **1996**, *29*, 933–939. (b) Politis, J. K.; Nemes, J. C.; Curtis, M. D. *J. Am. Chem. Soc.* **2001**, *123*, 2537.

(10) (a) Ong, B. S.; Wu, Y.; Liu, P.; Gardner, S. *J. Am. Chem. Soc.* **2004**, *126*, 3378–3379. (b) DeLongchamp, D. M.; Sambasivan, S.; Fischer, D. A.; Lin, E. K.; Chang, P.; Murphy, A. R.; Fréchet, J. M. J.; Subramanian, V. *Adv. Mater.* **2005**, *17*, 2340–2344. (c) Kim, D.; Han, J.; Park, Y.; Jang, Y.; Cho, J.; Hwang, M.; Cho, K. *Adv. Mater.* **2006**, *18*, 719–723.

(11) (a) Kline, R. J.; DeLongchamp, D. M.; Fischer, D. A.; Lin, E. K.; Richter, L. J.; Chabinyc, M. L.; Toney, M. F.; Heeney, M.; McCulloch, I. *Macromolecules* **2007**, *40*, 7960–7965. (b) Lucas, L. A.; DeLongchamp, D. M.; Vogel, B. M.; Lin, E. K.; Fasolka, M. J.; Fischer, D. A.; McCulloch, I.; Heeney, M.; Jabbour, G. E. *Appl. Phys. Lett.* **2007**, *90*, 012112.

(12) (a) Sirringhaus, H.; Wilson, R. J.; Friend, R. H.; Inbasekaran, M.; Wu, W.; Woo, E. P.; Grell, M.; Bradley, D. D. C. *Appl. Phys. Lett.* **2000**, *77*, 406. (b) Zen, A.; Pflaum, J.; Hirschmann, S.; Zhuang, W.; Jaiser, F.; Asawapirom, U.; Rabe, J.; Scherf, U.; Neher, D. *Adv. Funct. Mater.* **2004**, *14*, 757–764. (c) Cho, S.; Lee, K.; Yuen, J.; Wang, G.; Moses, D.; Heeger, A. J.; Surin, M.; Lazzaroni, R. *J. Appl. Phys.* **2006**, *100*, 114503. (d) Kim, F. S.; Guo, X.; Watson, M. D.; Jenekhe, S. A. *Adv. Mater.* **2010**, *22*, 478–482.